Development, characterization and application of an improved online reactive oxygen species analyzer based on MARGA

Jiyan Wu[1,2], Chi Yang[1,2], Chunyan Zhang [1,2], Fang Cao[1,2], Aiping Wu[1,2], Yanlin Zhang[1,2]

*

[1] *Yale-NUIST Center on Atmospheric Environ., Joint International Research Laboratory of Climate and Environment Change (ILCEC), Nanjing University of Information Science and Technology, Nanjing 210044, China*

[2] *School of Applied Meteorology, Nanjing University of Information Science and Technology, Nanjing 210044, China*

Correspondence: Yanlin Zhang (zhangyanlin@nuist.edu.cn)

Abstract

Excessive reactive oxygen species (ROS) in the human body is an important factor leading to diseases. Therefore, research on the content of reactive oxygen species in atmospheric particles is necessary. In recent years, the online detection technology of ROS has been developed. However, there are few technical studies on online detection of ROS based on the DTT method. Here, to modify the instrument, it is added a DTT experimental module that is protected from light and filled with nitrogen at the end, based on the Monitor for AeRosols and Gases in ambient Air (MARGA). The experimental study found that the detection limit of the modified instrument is 0.024 nmol min^{-1}. The DTT consumption rate of blank sample (ultra-pure water) is reduced by 44 %, which eliminates the influence of outside air and light in the experiment. And the accuracy of the online instrument is determined by comparing the online and offline levels of the samples, which yielded good consistency (slope 0.97, R^2=0.95). It shows that the performance of the instrument is indeed optimized, the instrument is stable, and the characterization of ROS is accurate. The instrument not only realizes the online detection conveniently and quickly, but also achieves the hour-by-hour detection of ROS based on the DTT method. Meanwhile, reactive oxygen and inorganic ions in atmospheric particles are quantified using the online technique in the northern suburbs of Nanjing. It is found that the content of ROS during the day is higher than that at night, especially after it rains, ROS peaks appear in the two time periods of 08:00-10:00 and 16:00-18:00. In addition, examination of the online ROS and water-soluble ions (SO_4^{2-}, NO_3^-, NH_4^+, Na^+, Ca^{2+}, K^+), BC and polluting gases (SO_2, CO, O_3, NO, NO_x) measurements revealed that photo-oxidation and secondary formation processes could be important sources of aerosol ROS. This method breakthrough enables the quantitative assessment of atmospheric particulate matter ROS at the diurnal scale, providing an effective tool to study sources and environmental impacts of ROS.

1、Introduction

Air quality is a major issue affecting human health, and prolonged exposure to high ambient particulate concentrations can lead to a significant increase in the probability of respiratory and cardiovascular diseases, which can seriously impair human health (Delfino et al., 2005; Ghio et al., 2012; Pöschl and Shiraiwa, 2015). The

43 production of reactive oxygen species (ROS) in the human body is the most reliable
44 pathophysiological mechanism proposed, and excessive reactive oxygen species can
45 cause an imbalance between the oxidative system and the antioxidant system, causing
46 oxidative stress and tissue damage (Ahmad et al., 2021; Akhtar et al., 2010; Borm et al.,
47 2007; Delfino et al., 2013; Lodovici and Bigagli, 2011). Thus, oxidative potential (OP)
48 has been proposed as a more biologically relevant indicator than particulate matter (PM)
49 mass concentration to represent the combined effects of multiple toxic components in
50 PM (Ayres et al., 2008; Hellack et al., 2015; Janssen et al., 2015). Understanding the
51 generation mechanism and source characteristics of reactive oxygen species is essential
52 for making reasonable pollution control decisions and reducing their impact on human
53 health.

54   In recent years, the analysis method of oxidation potential has cell detection and
55 cell-free detection. To provide a simpler and quicker way to determine the oxidation
56 potential of environmental particulate matter, cell-free methods such as electron spin
57 (or paramagnetic) resonance (OP_{ESR}), dithiothreitol assay (OP_{DTT}), ascorbic acid assay
58 (OP_{AA}), high-performance liquid chromatography (HPLC) and glutathione assay
59 (OP_{GSH}) are often used as the main measurement methods for ROS (Bates et al., 2019;
60 Ghio et al., 2012). Through the comparison and analysis of these various methods by a
61 large number of researchers, the DTT method is generally considered to be the most
62 common and comprehensive method to reflect the magnitude of the chemical oxidation
63 potential of particulate matter (Hedayat et al., 2014; Xiong et al., 2017).

64   Generally, the cell-free method still has problems with detection delays and
65 degradation of particulate chemical components during sample storage, which not only
66 leads to inaccurate detection data, but also the inability to capture daily changes.
67 Therefore, the development of online detection technology becomes necessary
68 (Charrier et al., 2016; Dou et al., 2015; Fang et al., 2017; Li et al., 2012; Liu et al., 2014;
69 Velali et al., 2016; Vreeland et al., 2017). So far, the development of online detection
70 technology is mainly based on the DCFH method and the DTT method. On the one
71 hand, an online detection technology based on the DCFH method has been reported
72 previously (Eiguren-Fernandez et al., 2017; Huang et al., 2016; Sameenoi et al., 2012;
73 Wragg et al., 2016). However, some researchers believe that in the DCFH method, the
74 horseradish peroxidase (HRP) will promote the production of hydroxyl free radicals,
75 leading to an overestimation of ROS content (Pal et al., 2012). On the other hand, based
76 on the DTT method to develop online detection technology (Fang et al., 2014;
77 Puthussery et al., 2018), The semi-automatic detection system researched by Fang et al,
78 based on the DTT method cannot realize an online collection of environmental samples.
79 On this basis, Puthussery et al used a mist chamber (MC) to continuously collect $PM_{2.5}$
80 in environmental water and realized fully automatic hourly ROS detection.

81   However, these detection methods ignore the influence of air and light on the
82 experiment. As the main reagent of the experiment, dithiothreitol (DTT) and 5,5'-
83 dithiobis (2-nitrobenzoic acid) (DTNB) are easily oxidized by air (Chen et al., 2010).
84 We achieve accurate measurement of the oxidation potential of environmental
85 particulates by shielding from light and filling with nitrogen. In addition, the present
86 study is developed on the basis of the MARGA, which is a state-of-art instrument.

MARGA measures near-real-time water-soluble particulate species and their gaseous precursors (Chen et al., 2017). MARGA is used to collect particulate matter and is connected to the optimized DTT_V detection part to observe the oxidation potential hour by hour. The system realizes simultaneous observation of oxidation potential and inorganic ions. Here, we optimize the performance of the instrument and measure the hourly averaged OP of ambient $PM_{2.5}$. The reliability of online detection of oxidation potential data is supported by analyzing the correlation between ions, polluting gases, BC and oxidation potential.

2、Materials and Method

2.1 Instrument set-up and improvement

Figure 1 shows the scheme and schematic diagram of the system for DTT online detection. The instrument is set up in the Atmospheric Environ. monitoring laboratory on the roof of the Wende Building of Nanjing University of Information Engineering (30 m above the ground) and the room temperature is maintained at 20°C. The entire system is composed of the MARGA, the automatic sample-receiving device, and the DTT experimental reaction device. The MARGA is used as an instrument for detecting atmospheric aerosols and inorganic components of gases (water-soluble ions Cl^-、NO_3^-、SO_4^{2-}、NH_4^+、Na^+、K^+、Mg^{2+}、Ca^{2+}), and it collects gases using a wet rotary separator and aerosols using steam injection, and absorbs gases and aerosols into the aqueous phase separately to separate them from each other. Then, the resulting solution is analyzed by ion chromatography equipped with a conductivity detector. That is, the gas and aerosol are analyzed separately to detect the gas precursors and different ionic compositions in the aerosol.

In past studies, MARGA was often used to detect the content of inorganic components of atmospheric aerosols and gases in cities around the world (Rumsey et al., 2014). And Chen et al. conducted a special evaluation study on the accuracy and precision of MARGA (Chen et al., 2017). In addition, Stieger et al. achieved quantitative analysis of low molecular weight organic acids in the atmospheric gas phase and particle phase by modifying MARGA (Stieger et al., 2019). Hemmilä et al used a MARGA ligation an electrospray ionization quadrupole mass spectrometer (MS) to achieve 1-hour resolution quantification of 7 different amines in gas and particulate phases in forest air in northern Finland. (Hemmilä et al., 2018) As a mature commercial instrument, MARGA can measure the inorganic components of atmospheric aerosols and gases with 1-hour resolution. In this study, based on MARGA, the DTT experimental part is connected to realize the hour-by-hour simultaneous detection of aerosol inorganic components and ROS.

In the DTT reaction module, to avoid the influence of light and air on the experiment, all pipelines, reaction flasks and mixing flasks are sealed and protected from light by aluminum foil. The whole DTT experimental part was filled with N_2 by pump A and pump B before the experiment started. In addition, we added a refrigerator to store DTT, DTNB and other experimental solutions. During the DTT experiment, the reaction tube and mixing tube were placed in an incubator at 37°C to simulate the temperature of human lungs. To realize the subsequent DTT experimental reactions, as

130 in Figure 1 we collected the liquid-phase aerosols into sample tubes through a dual-
131 channel split-flow controlled-volume peristaltic pump. And set peristaltic pump 1 speed
132 to 1.55 ml h^{-1} to finish 1.5 ml h^{-1} sample volume.

133 Finally, the determination of DTT activity is achieved by the continuous regular
134 operation of the programmable pumps A and B and the detection of the
135 spectrophotometer. (see Sect. 2.2.1 for details)

136 **2.2 Method**

137 **2.2.1 Online DTT assay measurement**

138 The whole measurement step is divided into three steps: sample collection, DTT
139 reaction part, and spectrophotometer detection. In the first step (the sample collection),
140 the MARGA will discharge 25 ml of aerosol liquid every hour, and use the dual-channel
141 split flow control volume peristaltic pump 1 to add 1.55 ml of the solution (to ensure
142 1.5 ml of sample) into the sample tube, and the rest will enter the automatic sampling
143 device to save through the peristaltic pump 2 (the automatic sampler is set to rotate one
144 grid per hour).

145 In the second step (the part is protected from light and in a nitrogen environment),
146 the reaction part is divided into a DTT oxidation step and a DTT determination
147 step(Wang et al., 2019). First (DTT oxidation step), use pump A to add 5 mL potassium
148 phosphate buffer (0.1 mol L^{-1}), 1.5 mL aerosol extract sample, and 0.5 mL DTT (1
149 mmol L^{-1}) into the mixing bottle (MV) in sequence. Inhale ultrapure water to clean the
150 syringe of pump A. DTT reacts with the aerosol extract in MV.

151 Second (DTT determination step), after completing the first step, at 0.10.20.30.40
152 minutes, use pump A to draw 1ml mixed solution in the mixing bottle and add it to the
153 reaction bottle. Then, immediately add 1 mL TCA (10% w/v; quencher) to the reaction
154 vial (RV, wrapped in aluminum foil to prevent possible light interference) using pump
155 A. Add 0.05 mL DTNB (1 mmol L^{-1}) via pump B and mix. The residual DTT reacts
156 with DTNB to form light absorption product 2-nitro-5-thiobenzoic acid (TNB) with
157 high extinction performance at 412 nm.

158 In the third step, in the detection part of the spectrophotometer, use pump A to add
159 4 mL Tris buffer (0.4 mol L^{-1}, containing 20 mmol L^{-1} EDTA) into the reaction flask
160 (RV). After the reaction is completed, use pump A to add the final mixture solution in
161 the reaction flask to the LWCC for the absorbance test. The data acquisition software
162 (Spectra Suite) records the absorbance at 412 and 700 nm every 10 min (select the
163 baseline absorbance of TNB). Then, the system uses deionized water (deionized water)
164 for self-cleaning to eliminate any residual liquid in the reaction flask, tubing, syringe,
165 and LWCC. To determine the rate of DTT consumption, the time interval is 10 min, and
166 a total of 6 (0 min, 10 min, 20 min, 30 min, 40 min, 50 min) data points of DTT
167 concentration over time are generated. Finally, the automated system performs the self-
168 cleaning procedure again to ensure that there is no residue, and the system repeats the
169 above operations in the next hour to realize hourly detection of DTT activity.

170
$$\Delta DTT = -\sigma Abs \cdot \frac{N_0}{Abs_0} \tag{1}$$

$$DTTv = \frac{\Delta DTT_s(nmol\ min^{-1}) - \Delta DTT_b(nmol\ min^{-1})}{V_t(m^3) \times \frac{V_s(mL)}{V_e(mL)}} \qquad (2)$$

where σAbs is the slope of absorbance versus time; Abs_0 is the initial absorbance calculated from the intercept of the linear regression of absorbance versus time; and N_0 is the initial moles of DTT added in the reaction vial. ΔDTT_s(nmol min⁻¹) is the DTT_v consumption rate of the sample, ΔDTT_b(nmol min⁻¹) is the blank DTT consumption rate, $V_t(m^3)$ is the sampling volume corresponding to the sample, and V_s(mL) is the injection volume, V_e(mL) is the sampling volume.

2.2.2 Online DTT instrument performance

The performance of the automated system is characterized by testing to determine the instrument response, limit of detection (LOD), precision and accuracy, while using a large flow sampler to collect samples for offline and online comparative analysis. (See Sect.3.1 for details)

We perform DTT activity detection and comparison on samples collected by 9,10-phenanthraquinone(PQN)and offline high-flow samplers. First, we select PQN with concentrations of 0.01, 0.02, 0.025, 0.05, 0.085 nmol L⁻¹ to compare online and offline DTT activity detection to determine the error of online and offline experiments. The details of PQN analysis can be found in Supplement S1. Secondly, select 10 offline collected samples for online and offline comparison, and then combine the experimental error between online and offline determined by PQN (PQN online and offline orthogonal fitting) to analyze the accuracy of online and offline.

2.2.3 Instrument maintenance

The MARGA is calibrated using internal and external standards. The internal standard is a 10 mg L⁻¹LiBr solution. The external standard calibration is performed after replacing the anion and cation columns, and the replacement cycle is generally 4 to 5 months. At the same time, the MARGA system is cleaned with 1% hydrogen peroxide and 10% acetone solution, and the airflow is calibrated every two months. In the DTT experimental module, DTT and DTNB solutions are prepared every 4 days. Before each test, perform a comprehensive light and nitrogen bag inspection. To ensure the accuracy of the experimental data, a standard curve was measured before each experiment. The instrument pipeline is cleaned once a week, as shown in Figure 1. The programmable pump A and pump B are connected to the ultrapure water channel. During the cleaning process, all pipelines, reaction tubes and mixing tubes are cleaned.

2.3 Collection and preparation of environmental samples

The sampling point is located on the roof of the seventh floor of the Maintenance Branch (34°58′ N, 117°26′ E) of the Power Company, Yunlong District, Xuzhou City. The surrounding buildings mainly include auto repair shops, logistics centers, pharmaceutical factories, and large residential areas and farmland. A large flow PM$_{2.5}$ sampler (KC-6120) is used for continuous sampling, and a total of 10 samples are collected (October 21, 2018-October 31, 2018). When sampling, the flow rate is 1.0 m³ min⁻¹, and each sampling time is 24 h. In this study, we collected samples using quartz filters and stored them in a refrigerator at -26 °C. Before the start of the experiment, the collected samples were subjected to extraction processing, and a sample film with a

diameter of 16 mm is cut into a brown glass bottle, 5 ml ultrapure water is added to shake for 30 min, and filtered with a 0.22 μm PTFE syringe filter to remove insoluble substances.

3. Results and discussion

3.1 Instrument performance

3.1.1 Improvement of the instrument

As we all know, photo-oxidation promotes the generation of ROS (Fang et al., 2016; Visentin et al., 2016; Yang et al., 2014). In addition, during the measurement process, the ingress of air inside the instrument will also cause the DTT activity to increase. Therefore, before on-site deployment, the online DTT inspection instrument is optimized by filling in nitrogen gas and shielding the whole from light. And respectively detect the DTT consumption rate (ΔDTT) of 10 blanks (ultra-pure water) before and after optimization. As shown in Figure 3, before the system optimization, we found that the average ΔDTT measured by 10 blanks was 0.25 ± 0.04 nmol min^{-1}, and there is a big fluctuation. After optimization, the average ΔDTT is 0.14 ± 0.008 nmol min^{-1}, which is significantly lower than system optimization. Moreover, the standard deviation (0.008) is much smaller than Puthussery et al (0.08) and Fang et al (0.103) (Fang et al., 2014; Puthussery et al., 2018). It shows that air and light do promote the generation of ROS, and the nitrogen environment and avoiding light contribute to the stability of the system. The optimized system is more accurate in measuring the oxidation potential of environmental particulate matter. To further prove the optimization effect, the performance of the instrument is studied. (See Sect.3.1.4 for details)

3.1.2 Calibration of DTTv measurement and analysis system

In past studies, PQN is often used as a standard sample of atmospheric particulate matter (Charrier and Anastasio, 2011; Charrier and Anastasio, 2015; Xiong et al., 2017). At pH 7.0, almost 100% of DTT was transformed to DTT-Disulfide by the catalyst 9,10-PQ (Li et al., 2009). The analytical measurement part of the online DTT instrument is calibrated by measuring the DTT activity of PQN at different concentrations. As shown in Figure 4, the linear graph of DTT consumption rate and PQN concentration, which is after subtracting the blank DTT consumption rate. The online detection slope is 3.66 ± 0.26, and the coefficient $R^2=0.992$. During the on-site operation, PQN's online and offline testing is measured at least once a month to ensure online accuracy.

3.1.3 Limit of detection and precision

The limit of detection (LOD) of the system is defined as 3 times the standard deviation of the deionized water blank (N = 23), i.e., 0.024 nmol min^{-1}, which is significantly lower than the LOD of Puthussery et al. (0.24 nmol min^{-1}) and Fang et al. (0.31 nmol·min^{-1}). To ensure the accuracy of the system, the deionized water blank samples are taken once a day (14 days) during the sampling period, besides the 10 continuously measured during the optimization of the system.

Use deionized water to evaluate the accuracy of the environmental sample automation system and analyze the DTT activity. The low standard deviation (coefficient of variation, CV=5.61%) of 0.024 nmol min^{-1} indicates that the system has

256 sufficiently high accuracy for environmental samples.

3.1.4 Accuracy

258 The accuracy of the system is verified by comparing the DTT activity of the
259 positive control and environmental particulate samples obtained from the automated
260 method with the results obtained from the same experimental protocol performed
261 manually. (Cho et al., 2005)

262 Five concentrations of PQN solutions (0.01, 0.02, 0.025, 0.05, 0.085 nmol L^{-1}) are
263 run in the automatic system, which is very close to the results of the manual system (the
264 standard deviation of the automatic system is kept at 0.008 nmol min^{-1}, and the
265 coefficient of variation is 2.28 %; the standard of the manual system The difference is
266 0.0044 nmol min^{-1}, the coefficient of variation is 1.48 %). As shown in Figure 5, the
267 slope (manual/automatic) obtained by orthogonal fitting is 1.14, the intercept is 0.12,
268 and the correlation coefficient (R^2) is 0.997. The manual detection results are slightly
269 higher than the automatic detection results, we assume that this is due to the instrument
270 error caused by the complicated piping system of the online instrument. To ensure the
271 high accuracy of the online system and the offline system, as a further verification, we
272 used online and offline manual methods to conduct DTT activity analysis on ten
273 environmental particulate matter samples.

274 As shown in Figure 6, the online and offline analysis of the DTT activity of 10
275 ambient particles, the slope (manual/automatic) obtained by orthogonal fitting is 1.14,
276 the intercept is 0.19, and the correlation coefficient (R^2) is 0.954. We found that the real
277 samples tested also had slightly higher offline results than online results. This is similar
278 to our assumption. Therefore, we use the PQN online and offline DTT consumption
279 rate orthogonal fitting result as the system to correct the error, as shown in Figure 6,
280 through the offline and online orthogonal fitting of 10 environmental particulate matter
281 samples before and after the error correction. We found that the corrected results are
282 better (the slope is 0.97 closer to 1, the intercept is 0.05 closer to 0, R^2=0.954). The
283 good agreement between the two sampling systems indicates that the DTT
284 measurement of environmental samples has high overall accuracy. These tests also
285 proved the necessity of optimization.

3.2 DTT activity of ambient samples

287 The volume-normalized oxidation potential DTT$_V$ is used as an index of exposure
288 to inhaled air to point out the inherent ability of particles to deplete relevant antioxidants.
289 During the observation period, the daily change of DTT$_V$ in Nanjing is shown in Figure
290 7. The average DTT$_V$ is 0.83±0.38 nmol min^{-1} m^{-3}. Compared with Beijing's DTT$_V$ in
291 the spring of 2012 (urban area: 0.24 nmol min^{-1} m^{-3})(Liu et al., 2014; Wang et al., 2019).
292 and Zhejiang University's annual DTT$_V$ average of 0.62 nmol min^{-1} m^{-3}(Yu et al., 2019) ,
293 our results are on the high side; And compared with Peking University's 2015 annual
294 DTT$_V$ (12.26±6.82 nmol min^{-1} m^{-3}) (Perrone et al., 2016)and Guangzhou's In the winter
295 of 2017 (DTT$_V$: 4.67±1.06 nmol min^{-1} m^{-3}) and in the spring of 2018 (DTT$_V$: 4.45±1.02
296 nmol min^{-1} m^{-3}), our values are low, which may be related to the current season and
297 emission factors. In addition, we found that the rain during the sampling period caused
298 significant changes in the 24-hour DTT$_V$. To better understand the environmental
299 factors affecting DTT$_V$, hourly data obtained by running the instrument is composited

to obtain a diurnal profile of the DTT activity. As shown in Figure S2, the daily distribution of 24-hour DTT activities during the entire sampling period (a), before rain (b), during rain (c), and after rain (d) are divided. Figure S2(a) represents the hourly change of DTT_V during the entire sample period. We found that the highest value of DTT_V in a day occurs at 11-12 am, and DTT_V is greater during the day than at night, which is similar to the study by Puthussery et al. Before the rain, the average DTT_V was 0.81 ± 0.17 nmol min^{-1} m^{-3}. There is a peak at 10-12 am, but the overall situation is relatively flat, and there is no obvious difference between day and night. And the average value of DTT_V during the rain is 0.55 ± 0.10 nmol min^{-1} m^{-3}, which decreased significantly. There is no doubt that this is caused by rain settling the polluting components of the atmosphere. In contrast, there is significant daily activity in DTT_V following rain, with peaks occurring mainly between 8-10 am and 4-6 pm, and DTT_V is significantly higher during the day than at night, which is similar to the Puthussery study (Puthussery et al., 2018). However, there are no obvious diurnal variation in $PM_{2.5}$ mass concentration. Therefore, the diurnal variation of DTT activity is assumed to be mainly attributed from different emission sources at the site.

3.3 The correlation between $PM_{2.5}$ and polluting gases and ROS activity

To further study, the daily changes of DTT_V and its correlation with various emission sources on site. As shown in Figure 7, we measured the water-soluble ionic components of $PM_{2.5}$ (SO_4^{2-}, NO_3^-, NH_4^+, Na^+, Ca^{2+}, K^+), BC, and pollution gas (SO_2, CO, O_3, NH_3) content changes. The average concentration of $PM_{2.5}$ during the sampling period is 9.97 ± 6.53 ug m^{-3}, the average concentration of $PM_{2.5}$ before rain is 11.13 ± 7.21 ug m^{-3}, the average concentration of $PM_{2.5}$ after rain is 7.80 ± 4.18 ug m^{-3}. The concentration of $PM_{2.5}$ is a significant drop. In addition, as shown in Table 1, there are differences in the correlation between $PM_{2.5}$ and DTT_V before and after rain. Therefore, we suspect that the source of DTT_V is different before and after the rain. BC and the polluting gases SO_2, NO_x, NO_2, CO, Ca^{2+}, K^+, Mg^{2+} are often used as tracers of biomass burning, coal combustion, and dust storms. Compared with the early winter in the northern suburbs of Nanjing (Zhang et al., 2020), the levels of these substances decreased during the sampling period. It is similar to Liu and Zhang et al who concluded that biomass burning, coal combustion, and dust storms were not major sources of pollution in Nanjing during the summer(Guo et al., 2019; Liu et al., 2019; Zhang et al., 2020). In addition, there is no strong correlation between DTT_V and SO_2, NO_x, NO_2, and CO before and after the rain. Therefore, it can be judged that neither biomass burning, coal combustion nor dust is the main source affecting DTT_V. In contrast, we found that there is a significant difference between day and night in O_3 after rain, which is similar to the change of DTT_V, and after rain, DTT_V and O_3 show a strong correlation (r=0.624). After it rains, the O_3 content in the air environment increases. Under the action of the sun's ultraviolet rays, the O_3 is photodegraded to form active oxygen components such as OH radicals (Ehhalt and Rohrer, 2000; Rohrer and Berresheim, 2006).

To further confirm the influence of light on DTT_V, the day and night correlation analysis of substances related to photo-oxidation (NH_4^+, NO_3^-, SO_4^{2-}) and DTT_V is carried out. As shown in Table S2, we find that NH_4^+, NO_3^-, SO_4^{2-} and DTT_V are

344 significantly correlated during the day (r=0.434, r=0.461, r=0.263, P<0.01). As far as
345 we know, there is no evidence in the literature that water-soluble inorganic ions (NH_4^+,
346 NO_3^-, SO_4^{2-}) have redox activity in an aerobic environment(Calas et al., 2018;
347 Stevanovic et al., 2017). However, their correlation with DTT_V may be due to
348 collinearity with redox-active organic compounds, rather than actual contribution to the
349 oxidation potential of particles. We speculate that the high correlation may be related
350 to the photochemical reactions that occur during the day.

351 **4、Summary and conclusions**

352 This study proposes and characterizes an improved online active oxygen analyzer.
353 Compared with the previous research, the main improvements(Fang et al., 2014;
354 Puthussery et al., 2018). The optimization analysis is as follows: (1) The experimental
355 environment is processed to isolate the air and avoid light; (2) The sampling method
356 has changed. We use the MARGA online ion analyzer, which is more mature and stable.
357 Compared with before optimization, the standard deviation of the blank was
358 significantly smaller, Thus, the detection limit of the instrument (0.024 nmol min^{-1})
359 becomes smaller and more stable. The DTT consumption rate is reduced by 44 %,
360 which eliminates the influence of outside air and light in the experiment. And the
361 consistency between online and offline is improved (slope=0.97, R^2=0.95), the
362 accuracy of the system is higher.

363 By changing the DTT_V content hour by hour during the sampling period, we found
364 that the DTT activity during the day is higher than that at night, and it is especially
365 obvious after rain, which is mainly related to the increase in UV radiation during the
366 day after rain. In addition, we analyzed the correlation between water-soluble ions
367 (SO_4^{2-}, NO_3^-, NH_4^+, Na^+, Ca^{2+}, K^+), BC, pollutant gases(SO_2, CO, O_3, NO, NO_x, NH_3)
368 and DTT_V, and we found that the main source of influence of OP in the Nanjing
369 environment in summer is daytime Secondary photochemical conversion and
370 ultraviolet radiation. In the future, we hope to add more experimental modules to the
371 back-end based on the MARGA sample collection device to realize the diversification
372 of detection compositions. In addition, the system can be combined with other
373 substance detection instruments. It will achieve the daily contribution of various
374 emission sources to the risk associated with OP exposure can be inferred from other
375 species.

376

377 *Data availability.* Data used in this paper can be provided upon request by email to
378 ZYL (dryanlinzhang@outlook.com) .

379 *Author contributions*. WJY designed the instrument, led the sampling campaign,
380 performed the experiments, and wrote the manuscript. YC participated in experimental
381 design and guided the experimental process. ZCY chose the building address and
382 initially built the instrument. CF helped in the filter collection and in conducting the
383 DTT activity experiments. ZYL conceived the idea, organized the manuscript, and
384 supervised the project.

385 *Competing interests.* The authors declare that they have no conflict of interest.

386 *Acknowledgements.* The authors thank funding support from the National Nature
387 Science Foundation of China (Nos. 41977305), the Natural Science Foundation of
388 Jiangsu Province (No. BK20180040), the fund from Jiangsu Innovation &
389 Entrepreneurship Team.

390

References:

Ahmad, M., Yu, Q., Chen, J., Cheng, S., Qin, W., and Zhang, Y.: Chemical characteristics, oxidative potential, and sources of PM (2.5) in wintertime in Lahore and Peshawar, Pakistan, J Environ Sci (China), 102, 148-158, https://doi.org/10.1016/j.jes.2020.09.014, 2021.

Akhtar, U. S., McWhinney, R. D., Rastogi, N., Abbatt, J. P., Evans, G. J., and Scott, J. A.: Cytotoxic and proinflammatory effects of ambient and source-related particulate matter (PM) in relation to the production of reactive oxygen species (ROS) and cytokine adsorption by particles, Inhal Toxicol, 22 Suppl 2, 37-47, https://doi.org/10.3109/08958378.2010.518377, 2010.

Ayres, J. G., Borm, P., Cassee, F. R., Castranova, V., Donaldson, K., Ghio, A., Harrison, R. M., Hider, R., Kelly, F., Kooter, I. M., Marano, F., Maynard, R. L., Mudway, I., Nel, A., Sioutas, C., Smith, S., Baeza-Squiban, A., Cho, A., Duggan, S., and Froines, J.: Evaluating the toxicity of airborne particulate matter and nanoparticles by measuring oxidative stress potential--a workshop report and consensus statement, Inhal Toxicol, 20, 75-99, https://doi.org/10.1080/08958370701665517, 2008.

Bates, J. T., Fang, T., Verma, V., Zeng, L., Weber, R. J., Tolbert, P. E., Abrams, J. Y., Sarnat, S. E., Klein, M., Mulholland, J. A., and Russell, A. G.: Review of Acellular Assays of Ambient Particulate Matter Oxidative Potential: Methods and Relationships with Composition, Sources, and Health Effects, Environ. Sci. Technol., 53, 4003-4019, https://doi.org/10.1021/acs.est.8b03430, 2019.

Borm, P. J. A., Kelly, F., Künzli, N., Schins, R. P. F., and Donaldson, K.: Oxidant generation by particulate matter: from biologically effective dose to a promising, novel metric, Occup Environ Med, 64, 73-74, https://doi.org/10.1136/oem.2006.029090, 2007.

Calas, A., Uzu, G., Kelly, F. J., Houdier, S., Martins, J. M. F., Thomas, F., Molton, F., Charron, A., Dunster, C., Oliete, A., Jacob, V., Besombes, J. L., Chevrier, F., and Jaffrezo, J. L.: Comparison between five acellular oxidative potential measurement assays performed with detailed chemistry on PM10 samples from the city of Chamonix (France), Atmos. Chem. Phys., 18, 7863-7875, https://doi.org/10.5194/acp-18-7863-2018, 2018.

Charrier, J. G. and Anastasio, C.: Impacts of Antioxidants on Hydroxyl Radical Production from Individual and Mixed Transition Metals in a Surrogate Lung Fluid, Atmospheric Environ. (Oxford, England : 1994), 45, 7555-7562, https://doi.org/10.1016/j.atmosenv.2010.12.021, 2011.

Charrier, J. G. and Anastasio, C.: Rates of Hydroxyl Radical Production from Transition Metals and Quinones in a Surrogate Lung Fluid, Environ. Sci. Technol., 49, 9317-9325, https://doi.org/10.1021/acs.est.5b01606, 2015.

Charrier, J. G., McFall, A. S., Vu, K. K. T., Baroi, J., Olea, C., Hasson, A., and Anastasio, C.: A bias in the "mass-normalized" DTT response – An effect of non-linear concentration-response curves for copper and manganese, Atmospheric Environ., 144, 325-334, https://doi.org/10.1016/j.atmosenv.2016.08.071, 2016.

Chen, X., Walker, J. T., and Geron, C.: Chromatography related performance of the Monitor for AeRosols and GAses in ambient air (MARGA): laboratory and field-based evaluation, Atmos. Meas. Tech., 10, 3893-3908, 10.5194/amt-10-3893-2017, 2017.

Chen, X., Zhong, Z., Xu, Z., Chen, L., and Wang, Y.: 2',7'-Dichlorodihydrofluorescein as a fluorescent probe for reactive oxygen species measurement: Forty years of application and controversy, Free Radic Res, 44, 587-604, https://doi.org/10.3109/10715761003709802, 2010.

Cho, A. K., Sioutas, C., Miguel, A. H., Kumagai, Y., Schmitz, D. A., Singh, M., Eiguren-Fernandez, A., and Froines, J. R.: Redox activity of airborne particulate matter at different sites in the Los Angeles Basin, Environ. Res., 99, 40-47, https://doi.org/10.1016/j.envres.2005.01.003, 2005.

Delfino, R. J., Sioutas, C., and Malik, S.: Potential role of ultrafine particles in associations between airborne particle mass and cardiovascular health, Environ. Health Perspect., 113, 934-946, https://doi.org/10.1289/ehp.7938, 2005.

Delfino, R. J., Staimer, N., Tjoa, T., Gillen, D. L., Schauer, J. J., and Shafer, M. M.: Airway inflammation and oxidative potential of air pollutant particles in a pediatric asthma panel, J Expo Sci Environ Epidemiol, 23, 466-473, https://doi.org/10.1038/jes.2013.25, 2013.

Dou, J., Lin, P., Kuang, B.-Y., and Yu, J.: Reactive Oxygen Species Production Mediated by Humic-like Substances in Atmospheric Aerosols: Enhancement Effects by Pyridine, Imidazole, and Their Derivatives, Environ. Sci. Technol., 49, https://doi.org/10.1021/es5059378, 2015.

Ehhalt, D. H. and Rohrer, F.: Dependence of the OH concentration on solar UV, J. Geophys. Res.: Atmospheres, 105, 3565-3571, https://doi.org/10.1029/1999jd901070, 2000.

Eiguren-Fernandez, A., Kreisberg, N., and Hering, S.: An online monitor of the oxidative capacity of aerosols (o-MOCA), Atmos Meas Tech, 10, 633-644, https://doi.org/10.5194/amt-10-633-2017, 2017.

Fang, T., Guo, H., Zeng, L., Verma, V., Nenes, A., and Weber, R. J.: Highly Acidic Ambient Particles, Soluble Metals, and Oxidative Potential: A Link between Sulfate and Aerosol Toxicity, Environ. Sci. Technol., 51, 2611-2620, https://doi.org/10.1021/acs.est.6b06151, 2017.

Fang, T., Verma, V., Guo, H., King, L., Edgerton, E., and Weber, R.: A semi-automated system for quantifying the oxidative potential of ambient particles in aqueous extracts using the dithiothreitol (DTT) assay: Results from the Southeastern Center for Air Pollution and Epidemiology (SCAPE), Atmos Meas Tech Discussions, 7, 7245-7279, https://doi.org/10.5194/amtd-7-7245-2014, 2014.

Fang, T., Verma, V., Bates, J., Abrams, J., Strickland, M., Ebelt, S., Chang, H., Mulholland, J., Tolbert, P., Russell, A., and Weber, R.: Oxidative potential of ambient water-soluble PM$_{2.5}$ in the southeastern United States: contrasts in sources and health associations between ascorbic acid (AA) and dithiothreitol (DTT) assays, Atmospheric Chem. Phys., 16, https://doi.org/10.5194/acp-16-3865-2016, 2016.

Ghio, A. J., Carraway, M. S., and Madden, M. C.: Composition of air pollution particles and oxidative stress in cells, tissues, and living systems, J. Toxicol. Environ. Health. Part B, Critical reviews, 15, 1-21, https://doi.org/10.1080/10937404.2012.632359, 2012.

Guo, Z., Guo, Q., Chen, S., Zhu, B., Zhang, Y., Yu, J., and Guo, Z.: Study on pollution behavior and sulfate formation during the typical haze event in Nanjing with water soluble inorganic ions and sulfur isotopes, Atmos Res, 217, 198-207, https://doi.org/10.1016/j.atmosres.2018.11.009, 2019.

Hedayat, F., Stevanovic, S., Miljevic, B., Bottle, S., and Ristovski, Z.: Review – Evaluating the molecular assays for measuring the oxidative potential of particulate matter, Chem Ind Chem Eengq, 21, 31-31, https://doi.org/10.2298/CICEQ140228031H, 2014.

Hellack, B., Quass, U., Nickel, C., Wick, G., Schins, R. P. F., and Kuhlbusch, T. A. J.: Oxidative potential of particulate matter at a German motorway, Environ Sci Process Impacts, 17, 868-876, https://doi.org/10.1039/c4em00605d, 2015.

Hemmilä, M., Hellén, H., Virkkula, A., Makkonen, U., Praplan, A. P., Kontkanen, J., Ahonen, L., Kulmala, M., and Hakola, H.: Amines in boreal forest air at SMEAR II station in Finland, Atmospheric Chem. Phys., 18, 6367-6380, 10.5194/acp-18-6367-2018, 2018.

Huang, W., Zhang, Y., Zhang, Y., Zeng, L., Dong, H., Huo, P., Fang, D., and Schauer, J. J.: Development of an automated sampling-analysis system for simultaneous measurement of reactive oxygen species (ROS) in gas and particle phases: GAC-ROS, Atmospheric Environ., 134, 18-26, https://doi.org/10.1016/j.atmosenv.2016.03.038, 2016.

479 Janssen, N. A., Strak, M., Yang, A., Hellack, B., Kelly, F. J., Kuhlbusch, T. A., Harrison, R. M.,
480 Brunekreef, B., Cassee, F. R., Steenhof, M., and Hoek, G.: Associations between three specific a-cellular
481 measures of the oxidative potential of particulate matter and markers of acute airway and nasal
482 inflammation in healthy volunteers, Occup Environ Med, 72, 49-56, https://doi.org/10.1136/oemed-
483 2014-102303, 2015.

484 Li, Q., Wyatt, A., and Kamens, R. M.: Oxidant generation and toxicity enhancement of aged-diesel
485 exhaust, Atmospheric Environ., 43, 1037-1042, 10.1016/j.atmosenv.2008.11.018, 2009.

486 Li, Y., Zhu, T., Zhao, J., and Xu, B.: Interactive enhancements of ascorbic acid and iron in hydroxyl
487 radical generation in quinone redox cycling, Environ. Sci. Technol., 46, 10302-10309,
488 https://doi.org/10.1021/es301834r, 2012.

489 Liu, Q., Baumgartner, J., Zhang, Y., Liu, Y., Sun, Y., and Zhang, M.: Oxidative potential and
490 inflammatory impacts of source apportioned ambient air pollution in Beijing, Environ. Sci. Technol., 48,
491 12920-12929, 10.1021/es5029876, 2014.

492 Liu, X., Zhang, Y. L., Peng, Y., Xu, L., Zhu, C., Cao, F., Zhai, X., Haque, M. M., Yang, C., Chang, Y.,
493 Huang, T., Xu, Z., Bao, M., Zhang, W., Fan, M., and Lee, X.: Chemical and optical properties of
494 carbonaceous aerosols in Nanjing, eastern China: regionally transported biomass burning contribution,
495 Atmos. Chem. Phys., 19, 11213-11233, https://doi.org/10.5194/acp-19-11213-2019, 2019.

496 Lodovici, M. and Bigagli, E.: Oxidative stress and air pollution exposure, J. Toxicol, 2011, 487074,
497 https://doi.org/10.1155/2011/487074, 2011.

498 Pal, A. K., Bello, D., Budhlall, B., Rogers, E., and Milton, D. K.: Screening for Oxidative Stress Elicited
499 by Engineered Nanomaterials: Evaluation of Acellular DCFH Assay, Dose Response, 10, 308-330,
500 https://doi.org/10.2203/dose-response.10-036.Pal, 2012.

501 Perrone, M. G., Zhou, J., Malandrino, M., Sangiorgi, G., Rizzi, C., Ferrero, L., Dommen, J., and
502 Bolzacchini, E.: PM chemical composition and oxidative potential of the soluble fraction of particles at
503 two sites in the urban area of Milan, Northern Italy, Atmospheric Environ., 128, 104-113,
504 https://doi.org/10.1016/j.atmosenv.2015.12.040, 2016.

505 Pöschl, U. and Shiraiwa, M.: Multiphase chemistry at the atmosphere-biosphere interface influencing
506 climate and public health in the anthropocene, Chemical reviews, 115, 4440-4475,
507 https://doi.org/10.1021/cr500487s, 2015.

508 Puthussery, J. V., Zhang, C., and Verma, V.: Development and field testing of an online instrument for
509 measuring the real-time oxidative potential of ambient particulate matter based on dithiothreitol assay,
510 Atmos. Meas. Tech., 11, 5767-5780, https://doi.org/10.5194/amt-11-5767-2018, 2018.

511 Rohrer, F. and Berresheim, H.: Strong correlation between levels of tropospheric hydroxyl radicals and
512 solar ultraviolet radiation, Nature, 442, 184-187, https://doi.org/10.1038/nature04924, 2006.

513 Sameenoi, Y., Koehler, K., Shapiro, J., Boonsong, K., Sun, Y., Collett, J., Jr., Volckens, J., and Henry, C.
514 S.: Microfluidic electrochemical sensor for on-line monitoring of aerosol oxidative activity, J. Am. Chem.
515 Soc., 134, 10562-10568, https://doi.org/10.1021/ja3031104, 2012.

516 Stevanovic, S., Vaughan, A., Hedayat, F., Salimi, F., Rahman, M. M., Zare, A., Brown, R. A., Brown, R.
517 J., Wang, H., Zhang, Z., Wang, X., Bottle, S. E., Yang, I. A., and Ristovski, Z. D.: Oxidative potential of
518 gas phase combustion emissions - An underestimated and potentially harmful component of air pollution
519 from combustion processes, Atmospheric Environ., 158, 227-235,
520 https://doi.org/10.1016/j.atmosenv.2017.03.041, 2017.

521 Stieger, B., Spindler, G., van Pinxteren, D., Grüner, A., Wallasch, M., and Herrmann, H.: Development
522 of an online-coupled MARGA upgrade for the 2 h interval quantification of low-molecular-

weight organic acids in the gas and particle phases, Atmos. Meas. Tech., 12, 281-298, https://doi.org/10.5194/amt-12-281-2019, 2019.

Velali, E., Papachristou, E., Pantazaki, A., Choli-Papadopoulou, T., Planou, S., Kouras, A., Manoli, E., Besis, A., Voutsa, D., and Samara, C.: Redox activity and in vitro bioactivity of the water-soluble fraction of urban particulate matter in relation to particle size and chemical composition, Environ. Pollut., 208, 774-786, https://doi.org/10.1016/j.envpol.2015.10.058, 2016.

Visentin, M., Pagnoni, A., Sarti, E., and Pietrogrande, M. C.: Urban $PM_{2.5}$ oxidative potential: Importance of chemical species and comparison of two spectrophotometric cell-free assays, Environ. Pollut., 219, 72-79, https://doi.org/10.1016/j.envpol.2016.09.047, 2016.

Vreeland, H., Weber, R., Bergin, M., Greenwald, R., Golan, R., Russell, A. G., Verma, V., and Sarnat, J. A.: Oxidative potential of PM2.5 during Atlanta rush hour: Measurements of in-vehicle dithiothreitol (DTT) activity, Atmospheric Environ., 165, 169-178, https://doi.org/10.1016/j.atmosenv.2017.06.044, 2017.

Wang, J., Lin, X., Lu, L., Wu, Y., Zhang, H., Lv, Q., Liu, W., Zhang, Y., and Zhuang, S.: Temporal variation of oxidative potential of water soluble components of ambient $PM_{2.5}$ measured by dithiothreitol (DTT) assay, Sci. Total Environ., 649, 969-978, https://doi.org/10.1016/j.scitotenv.2018.08.375, 2019.

Wragg, F. P. H., Fuller, S. J., Freshwater, R., Green, D. C., Kelly, F. J., and Kalberer, M.: An automated online instrument to quantify aerosol-bound reactive oxygen species (ROS) for ambient measurement and health-relevant aerosol studies, Atmos. Meas. Tech., 9, 4891-4900, https://doi.org/10.5194/amt-9-4891-2016, 2016.

Xiong, Q., Yu, H., Wang, R., Wei, J., and Verma, V.: Rethinking Dithiothreitol-Based Particulate Matter Oxidative Potential: Measuring Dithiothreitol Consumption versus Reactive Oxygen Species Generation, Environ. Sci. Technol., 51, 6507-6514, https://doi.org/10.1021/acs.est.7b01272, 2017.

Yang, A., Jedynska, A., Hellack, B., Kooter, I., Hoek, G., Brunekreef, B., Kuhlbusch, T. A. J., Cassee, F. R., and Janssen, N. A. H.: Measurement of the oxidative potential of $PM_{2.5}$ and its constituents: The effect of extraction solvent and filter type, Atmospheric Environ., 83, 35-42, https://doi.org/10.1016/j.atmosenv.2013.10.049, 2014.

Yu, S., Liu, W., Xu, Y., Yi, K., Zhou, M., Tao, S., and Liu, W.: Characteristics and oxidative potential of atmospheric $PM_{2.5}$ in Beijing: Source apportionment and seasonal variation, Sci. Total Environ., 650, 277-287, https://doi.org/10.1016/j.scitotenv.2018.09.021, 2019.

Zhang, C., Yang, C., Liu, X., Cao, F., and Zhang, Y.-l.: Insight into the photochemistry of atmospheric oxalate through hourly measurements in the northern suburbs of Nanjing, China, Sci. Total Environ., 719, 137416, https://doi.org/10.1016/j.scitotenv.2020.137416, 2020.

557
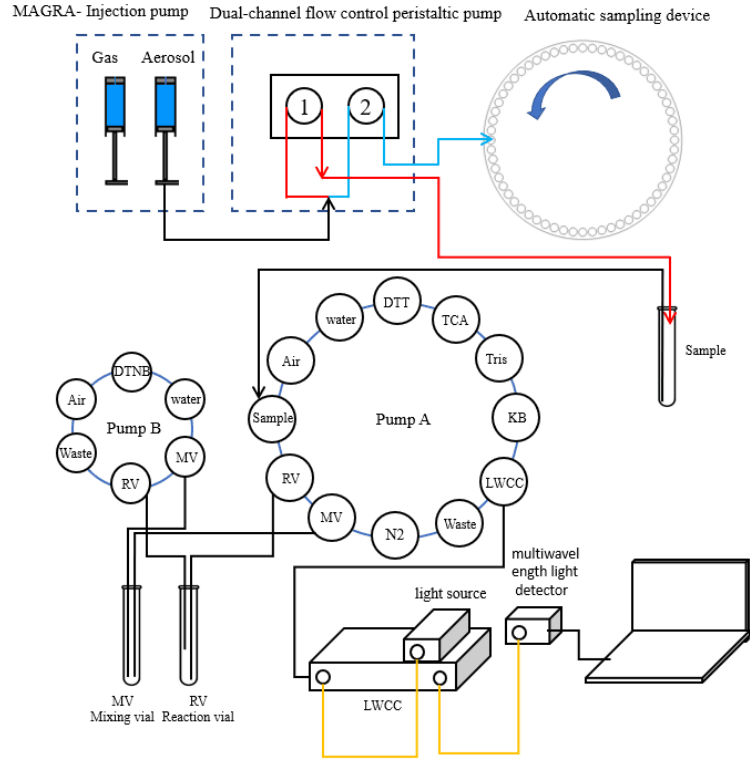
Figure 1. Automated system setup (Red line: Peristaltic pump 1 runs at a flow rate of 23 ml h^{-1} for the first 4 minutes of each hour; Blue line: Peristaltic pump 2 runs at a flow rate of 27 ml h^{-1} for the remaining 56 minutes of each hour; Yellow line: Optical fiber)

561
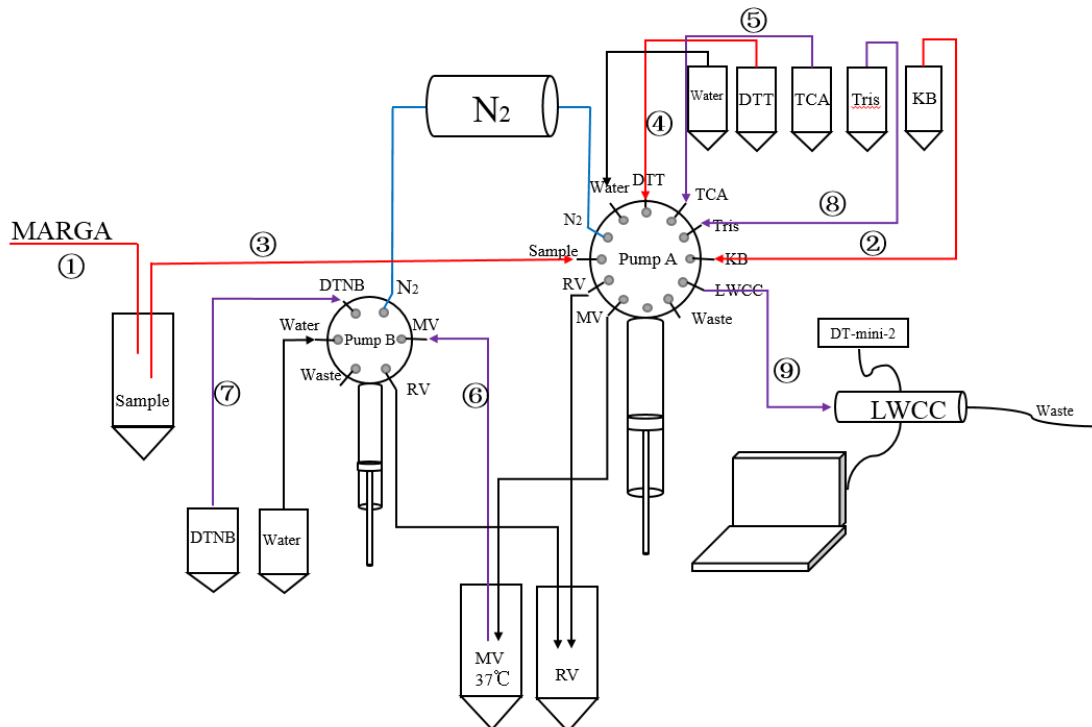
Figure.2 Schematic diagram of DTT reaction part. (①-④ represents the DTT oxidation step,⑤-⑨ represents the DTT determination step. Blue indicates the ventilation line, all pipelines are wrapped in aluminum foil to protect from light.)
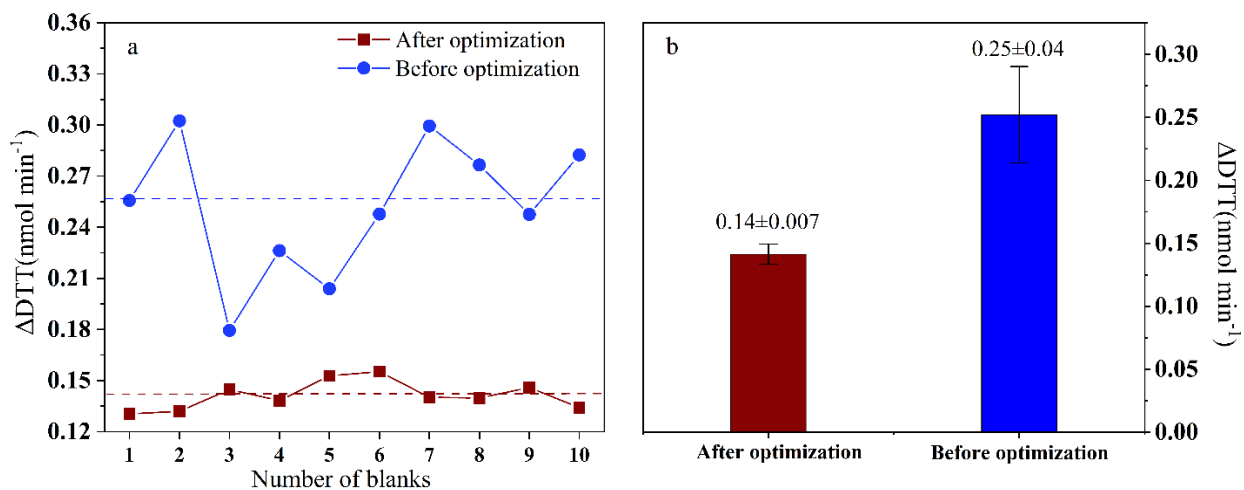
Figure 3. Comparison of blank DTT consumption rate and standard deviation after system optimization (the dotted line is the average value)
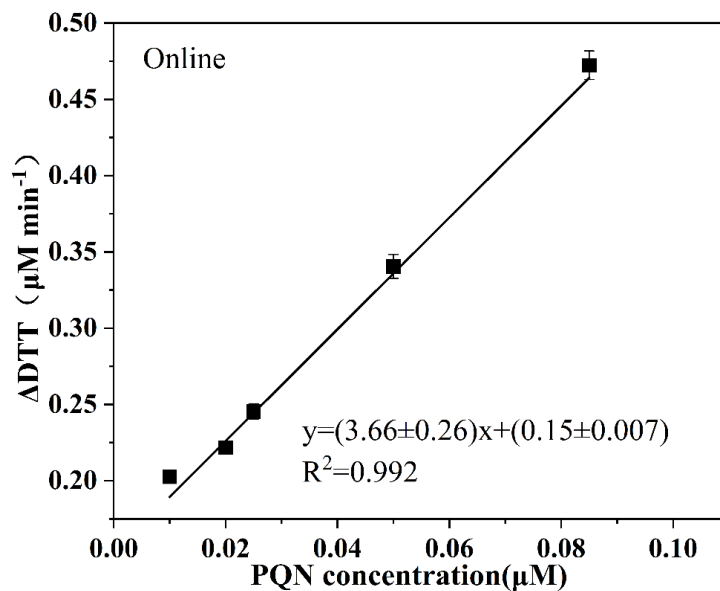
Figure 4. Blank corrected DTT consumption rate as a function of PQN used as a positive control. Each error bar represents the standard deviation of three independent DTT measurements on each concentration.

572
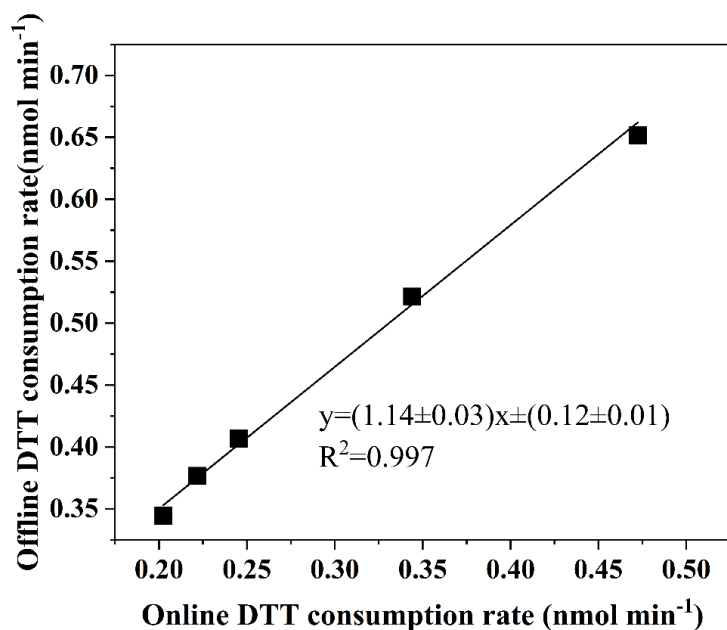
Figure 5. Comparison of the automated system with manual operation using PQN (9,10-phenanthraquinone)

575
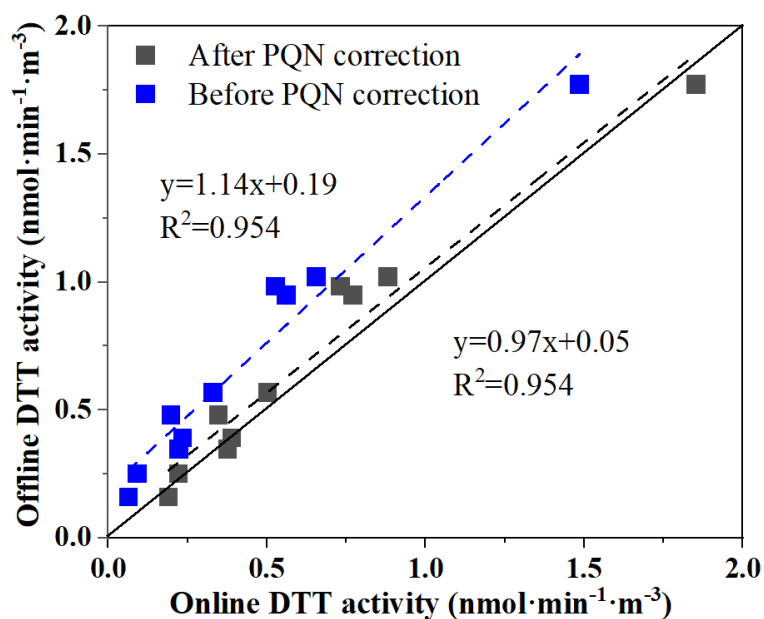
Figure 6. Comparison of the automated system with manual operation using ambient aerosol extracts (PM$_{2.5}$ samples collected from Xuzhou, regression analysis is done by orthogonal regression; the line is 1:1).

579
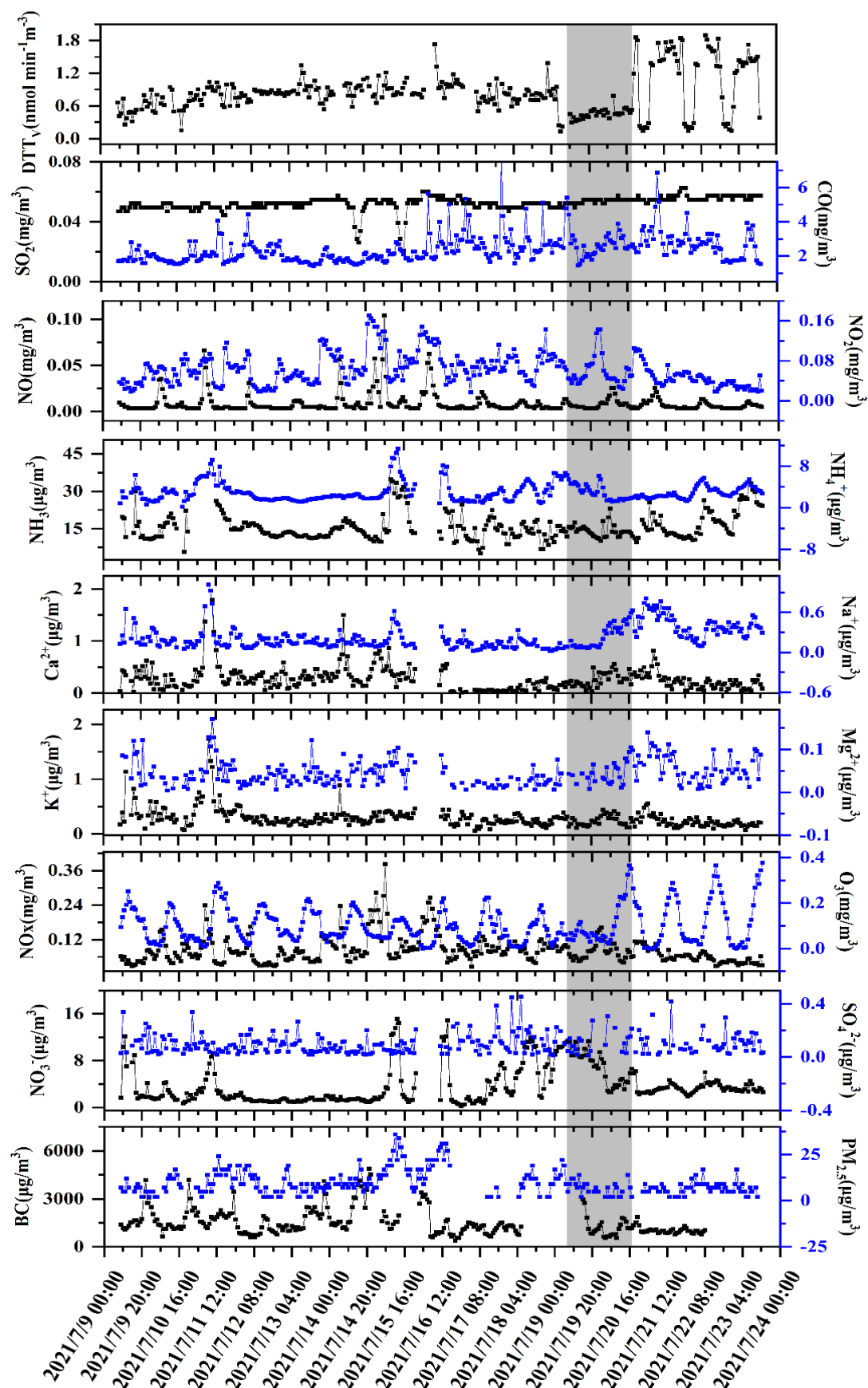
580
581 **Figure 7 .** Time series of the DTT activity, PM$_{2.5}$ water-soluble components (SO$_4^{2-}$, NO$_3^-$, NH$_4^+$,
582   Na$^+$, Ca^{2+}, K$^+$) and polluting gases (SO$_2$, CO, O$_3$, NH$_3$) (The shaded part is rainy weather)

583

Table 1. The correlation coefficient (R) between the concentration of water-soluble chemical substances in environmental $PM_{2.5}$ ($\mu g\ m^{-3}$) and the volume normalized substance concentration (DTT_V), before rain, during rain, and after rain.

Parameter	Total	Before it rains	During rain	After rain
$PM_{2.5}$	0.014	0.305**	0.026	-0.290*
SO_2	0.195**	0.114	-0.136	0.222
NO	-0.029	-0.029	-0.074	0.050
NO_2	-0.098	0.115	0.169	-0.203
NO_x	-0.085	0.062	0.142	-0.169
CO	-0.033	0.146*	-0.093	0.121
O_3	0.227*	0.153	0.044	0.624**
BC	-0.052	-0.054	-0.439*	0.087
NH_3	0.241**	0.074	-0.129	0.269*
SO_4^{2-}	-0.06	-0.065	0.329	0.028
NO_3^-	-0.163*	-0.155*	-0.352*	0.511**
NH_4^+	0.024	0.028	0.062	0.271*
K^+	-0.077	-0.045	0.125	-0.337**
Mg^{2+}	0.131*	0.075	0.233	0.086
Ca^{2+}	0.005	0.072	0.021	-0.055
Na^+	0.177**	-0.007	0.133	0.008

587    $PM_{2.5}$, particulate matter with an aerodynamic diameter $< 2.5\mu m$; *P<0.05, **P<0.01.

588